

## Photon Efficiency: Retrospective and Perspective

Petro P. Trokhimchuck\*

Anatoliy Svidzinskiy Department of Theoretical and Computer Physics, Lesya Ukrayinka Volyn' National University, 13 Voly Avenue, 43025, Lutsk, Ukraine

**\*Corresponding Author:** Petro P. Trokhimchuck, Anatoliy Svidzinskiy Department of Theoretical and Computer Physics, Lesya Ukrayinka Volyn' National University, 13 Voly Avenue, 43025, Lutsk, Ukraine

**Abstract:** Main peculiarities of photon efficiency are discussed. Short historical analysis of this problem is discussed. Questions about possible observation these phenomena in Chemistry, Classic, Nonlinear and Relaxed Optics are analyzed. Corresponding experimental data and models and theories, which are used for the explanation these phenomena, are represented.

**Keywords:** photon efficiency, Stark-Einstein law, laser irradiation, photochemistry, Nonlinear Optics, Relaxed Optics, phemtochemistry, cascade processes.

### 1. INTRODUCTION

The problem of effective use of optical radiation for observing the main processes and phenomena of the interaction of optical radiation with matter contributes to their deeper study. In this regard, it is advisable to introduce the concept of photonic (photochemical) efficiency, which is used in one form or another in chemistry, classical, Nonlinear, and Relaxed Optics.

Concept of the photochemical efficiency was introduced by A. Einstein [1-3] for the equilibrium case. But it must be developed in Laser Physics and Nonlinear Optics [4-6], Relaxed Optics [7-12] and chemistry [2, 13-20]. It must be universal concept.

In general, it makes sense to talk about differential and integral photon efficiency. The differential photon efficiency is introduced at the microlevel for each act of scattering (absorption) of a photon by a medium; integral at the macro level and characterizes macroscopic changes in the properties of the medium or radiated or both radiation and the medium. Appropriate models and theories should be created for each specific case.

According to the level of complexity and scope, photon efficiency can be classified as follows:

1. Radiative photon efficiency.
2. Non-radiative photon efficiency.
3. Mixed photon efficiency.
4. Cascade radiative photon efficiency.
5. Cascade nonradiative photon efficiency.
6. Cascade mixed photon efficiency.

An example of the radiative photon efficiency is the optical pumping of lasers [5, 6, 21], and the nonradiative efficiency is photochemical reactions [2]. The mixed photon efficiency characterizes the optical pumping of a laser with heating of the active medium and autooscillative chemical reactions of Belousov-Zhabotinskiy type) [15-17].

Nonlinear optical phenomena are characterized by cascade photon radiative efficiency [4]. Chain chemical reactions [14] and some chains of relaxed-optical processes [7, 9] are represented cascade photon non-radiative efficiency. A number of chains of relaxed-optical processes are characterized by a cascade mixed photon efficiency [7, 9, 12].

An example of a mixed optical-electronic system is a photomultiplier tube [22]. It is an electrovacuum device in which the electron flow emitted by a photocathode under the action of optical radiation (photocurrent) is amplified in the multiplier system as a result of secondary electron emission; the

current in the anode circuit (collector of secondary electrons) significantly exceeds the initial photocurrent (usually  $10^5$  times or more). Only first stage of cascade has optical nature.

The integral photochemical (photon) efficiency is connected associated with the direct transformation of the photon flux into photochemical transformations in the irradiated material. It is directly related to differential efficiency. But there is one subtlety in the absorption of radiation by unstable or metastable centers (disordered and amorphous media): the exposure time does not play a big role. At the same time, the radiation saturation mode is of great importance for crystals. For radiative relaxation we have luminescence, generation of laser radiation and various nonlinear optical phenomena; for nonradiative relaxation – relaxed-optical phenomena (phase transformations of the irradiated medium).

To increase the photon efficiency, the space-time conditions of irradiation also play an important role. For Nonlinear Optics, they are closely related to coherence and are called phase-matching conditions [4]; for Relaxed Optics, the concept of coherent structures can be used [9].

## 2. CLASSIC PHYSICS AND CHEMISTRY

The concept of differential photochemical efficiency is connected related to the photochemical equivalent law [1, 2]. According to A. Einstein, there is the following relationship between photochemical phenomena and the radiation that causes them: in any elementary photochemical process of dissociation of a molecule under the action of radiation, the energy required for the process is equal to  $h\nu$  [1]. This law for sufficiently weak radiation fluxes was derived by A. Einstein on the basis of thermodynamic reasoning.

This conclusion was based on five hypotheses [1]:

1. If the gas is exposed to radiation with frequencies belonging to the interval  $d\nu$ , which is part of the region of the spectrum to which the reaction under consideration is sensitive, then the number of molecules that decay per unit time is proportional to the radiation intensity and the number of available AB molecules (diatomic molecules are chosen for simplicity). The energy  $\varepsilon$  of the light absorbed during the splitting of one gram-molecule of AB does not depend on the radiation intensity, but may depend on the radiation frequency and gas temperature.
2. The only result of the interaction of radiation and gas is photochemical processes, so that the transition of energy  $\varepsilon$  from radiation with frequency  $\nu$  to gas is unambiguously (as by a rigid mechanism) associated with the splitting of the AB gram molecule.
3. The number of recombinations of molecules A and B per unit time does not depend does not depend on the radiation density.
4. The energy of radiation corresponding to a certain frequency interval  $d\nu$ , released during the recombination of one gram molecule A and one gram molecule B, does not depend on the radiation density.

In contrast to A. Einstein's model, we have more intense radiation fluxes and, depending on the irradiation conditions, we can have such nonlinear optical phenomena as quantum splitting, multiphoton absorption, etc.

The ratio of the number of molecules involved in a photochemical reaction to the number of absorbed light quanta is called the quantum yield of the photochemical reaction.

According to [2, 3, 23] photoionization processes should be considered as chemical reactions.

Photoelectrochemical processes are processes in chemistry, they usually involve the conversion of light into other forms of energy [2, 3, 23]. These processes occur in photochemistry, optically inflated lasers, sensitized solar cells, luminescence and photochromism.

Stark-Einstein's law – one quantum of absorbed light causes one elementary chemical reaction [2]. The law allows establishing the relationship between the absorbed energy and the degree of transformation of matter.

It should be noted that in addition to single-photon ionization processes, there can be multiphoton ionization processes and associated dissociation. In this case, the Stark-Einstein law should be corrected.

For multiquantum excitation, two different mechanisms are possible [2]. Let us illustrate their action first for the case of two-photon absorption, and then we pass to multiphoton absorption.

The first mechanism consists in successively stepwise absorption of two photons through the real intermediate state of absorbing particles (Fig. 1a) [2]. It will be settled upon absorption of the first photon and is the starting point for the absorption of the second photon. The real intermediate state has a certain lifetime, usually  $10^{-4} - 10^{-9}$  s. The entire sequence of processes in the case of the first mechanism is called resonant two-stage excitation. The second excitation mechanism is non-resonant two-stage excitation, in which no real intermediate state participates [2]. When the first photon interacts with molecule A, the virtual state  $A^{**}$  is excited (Fig. 1b). The second photon can only be absorbed if it is absorbed during the absorption of the first (which is equivalent to one period of electromagnetic radiation, or  $10^{-15}$  s). Therefore, such a process is often called simultaneous two-photon absorption in contrast to successive stepwise absorption [2]. To implement such processes, a high intensity of irradiation is necessary. For a two-stage excitation process, it is required that the second stage occurs in a time shorter than the relaxation time of the first excitation (due to collisions, internal conversion, and emission) of particles from the intermediate state  $A^*$ , while in the case of a nonresonant two-photon process, two photons must be absorbed one after another in interval of  $10^{-15}$  s. The first process has a higher probability than the second, although these two mechanisms coincide if, in the approximation of a nonresonant process, the photon energy of the exciting radiation corresponds to the real intermediate state [2].

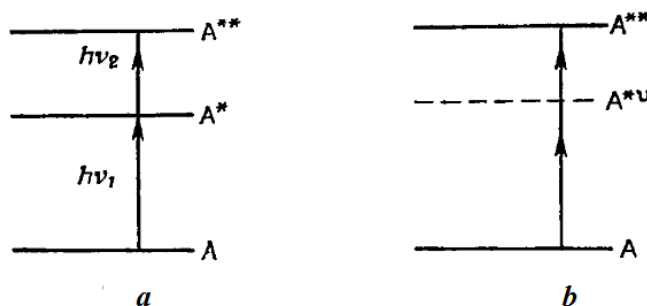


Fig1. Resonant (a) and nonresonant (b) two-photon absorption [2].

An important feature of multiquantum excitation mechanisms is the possibility of using the total energy of several photons, although for each individual photon the energy is quantized according to Planck's formula. Optical absorption now depends on the intensity of the incident radiation, while the Lambert-Baer law is not satisfied. This behavior is most understandable for a multiquantum excitation process involving virtual intermediate states. A system that is completely transparent to low irradiation intensity can absorb radiation of the same wavelength but at high intensity.

Since the basic elementary reaction that occurs when one quantum of light is absorbed is often accompanied by side reactions, the quantum yield differs from one.

Instead of the quantum yield of a reaction, we introduce a more general concept of differential photon efficiency. This value characterizes not only chemical reactions in the classical sense of the word, but also ionization, chemical bonds, coordination numbers, etc.

It should be noted that fractional quantum (photon) absorption can also occur. In this case, the photon energy  $h\nu$  should be more than twice the ionization (activation) energy  $E_a$  of the corresponding state.

Now we can formulate the *generalized Stark-Einstein law*: to break (ionize) a certain state, the total energy of a certain number of photons must be greater than or equal to the energy of the excited bond.

The mathematical form of writing for three absorption modes can be represented for the differential photon efficiency  $\delta$  in the following form:

- 1)  $\delta < 1$  for multi photon absorption;
- 2)  $\delta = 1$  for one-photon absorption;
- 3)  $\delta > 1$  for fractional photon absorption.

Roughly speaking, these three conditions are formalized presentation of generalized Stark-Einstein law.

For the research dynamics of chemical reactions we must have possibility to receive and use ultra short times. For resolution of these problems femtochemistry was created [13, 24].

Femtochemistry is a branch of physical chemistry that studies chemical reactions over very short time intervals, on the order of femtoseconds (hence the name). For his work in this area, A. Zewail received the Nobel Prize in Chemistry in 1999 [13]: "for real-time studies of chemical reactions using femtosecond spectroscopy." The main result of the work is that it became possible to observe the flow of elementary chemical reactions "in real time" and thereby created a new branch of chemistry - femtochemistry, which studies chemical processes in the femtosecond time range ( $10^{-15} - 10^{-12}$  seconds). Elementary reactions are studied in a special branch of chemistry – chemical dynamics. The main task of chemical dynamics is to determine the structure of the transition state and trace the dynamics of its formation and decay in real time.

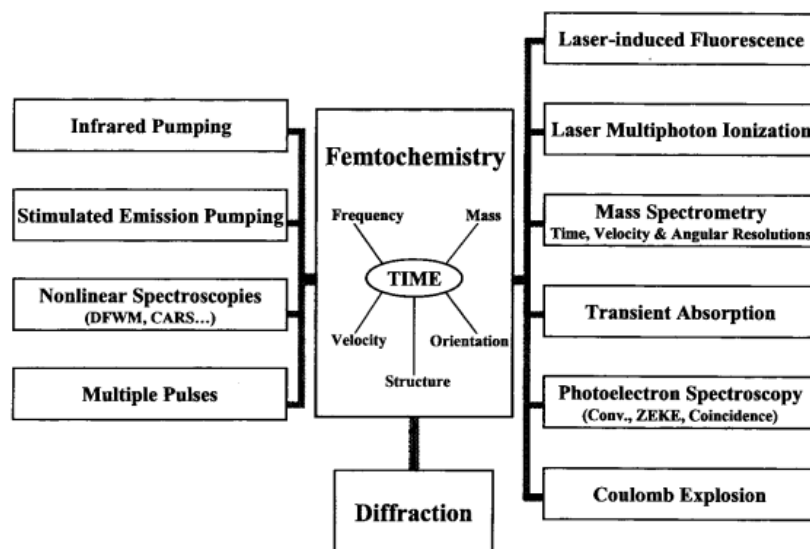


**Fig2.** Techniques for probing in phemtochemistry. Both exciter and ground states have been probes in this method. The correlations of time with frequency, mass velocity and orientatin were essential in the studies of complex systems. Diffraction represents the new effort for probing structures [13].

In whole, phemtochemistry allow to select pure photochemical processes between set of other (thermal chemical, various mixing, etc.) [13, 24].

It should be noted that for the irradiation of indium antimonide by ruby laser radiation, the lower limit of the time interval is  $10^{-7} - 10^{-5}$  seconds. From this point of view, femtochemistry can also be considered as a branch of Relaxed Optics [3, 7, 9].

Photochemical processes also make a great contribution to chemical chain reactions. Let us illustrate this by the example of the formation of phosgene  $\text{CO} + \text{Cl}_2 = \text{COCl}_2$  [14].

The photochemical reaction proceeds well under visible light in glass vessels. The presence of oxygen inhibits the reaction, and part of the CO is oxidized to  $\text{CO}_2$ . When the amount of oxygen is large enough to completely oxidize CO, then in practice only the oxidation of CO to  $\text{CO}_2$  occurs, while phosgene is almost not formed at all. In this case,  $\text{Cl}_2$  is consumed and plays the role of a sensitizer.

Both the reaction of phosgene formation (in mixtures where there is no oxygen or where there is little of it) and the reaction of sensitized  $\text{CO}_2$  formation (in mixtures with high oxygen content) are valuable, since their quantum yield is very high: the quantum yield of the first reaction reaches 3000, and the second 1000 molecules per absorbed photon [14].

### 3. NONLINEAR OPTICS

We will consider nonlinear optical processes in various media, with special attention to solids. Classical Nonlinear Optical (NLO) processes may be split into two groups [4]:

1. Intense light field, which is commensurate with the intracrystalline field.
2. Weak electric field, but strong external fields (mechanical, electric, magnetic) are superimposed on the medium.

The first group of phenomena forms the basis of classical non-linear optics and arose with the development of laser physics. This group of phenomena includes optical pumping of lasers,

generation of harmonics, parametric generation of light, up and down conversion (Stokes and anti-Stokes processes), stimulated Raman and Brillouin scattering, electrostriction, self-focusing and self-trapping, etc.

The second group of phenomena is studied by parametric crystal optics. This group of phenomena includes the effects of Faraday, Pockels, Kerr; phenomena of electro- and magneto-optical gyration, etc.

According to I. Frank Cherenkov radiation may be represented as NLO phenomenon too [7].

From the electrodynamic point of view, the difference between classical nonlinear optical phenomena and Cherenkov radiation is as follows. Classical NLO phenomena are due to a homogeneous laser-induced polarization of the medium, and Cherenkov radiation is due to an induced inhomogeneous polarization of the irradiated substance [7].

We focus on the generation of harmonics (multiquantum processes). Multi-quantum ionization is obtained using an ultraviolet laser. The process is called resonantly enhanced multiquantum ionization if resonant intermediate states are involved in it. Single-photon ionization of most particles requires the use of radiation wavelengths that lie in the intrinsic absorption region of the irradiated material. The use of multiquantum irradiation makes it possible to increase the transmission region of the material and makes it possible to sharply increase the ionization of particles in the volume of the irradiated medium [2, 4].

Multiquantum effects under the action of ultraviolet or visible laser radiation are often similar to those excited by single-photon excitation by the corresponding short-wavelength radiation. However, infrared multi-quantum excitation leads to phenomena that would be impossible to observe without the use of lasers. Let us present data on the use of a CO<sub>2</sub> laser [2].

In most cases, the absorption of 10-40 IR photons is required to achieve bond breaking. When a molecule with a strong vibrational absorption band is exposed to high-power pulsed laser radiation, photofragmentation occurs relatively easily. So the SF<sub>6</sub> molecule dissociates when exposed to a CO<sub>2</sub> laser (wavelength 10.6 μm)



coinciding with the ν<sub>3</sub> band, although the binding energy of SF<sub>5</sub> - F is 348 kJ/mol, which is more than 30 times greater than the photon energy.

Schema one of model multiquantum dissociation is represented in Fig. 2 [2]. For beginning stages of the excitation (little energy) vibrational levels have discrete nature (region I). Absorption of first photon is generating the molecule excitation from zero level to first level. Next stages of excitation on levels 2, 3, 4, ...n can't be in resonance with initial laser radiation. In multiatom molecule the density of vibrational states is increased together with increasing of energy, and, beginning from some critical value region of discrete vibrational levels transit to quasicontinuum (region II of Fig. 2).

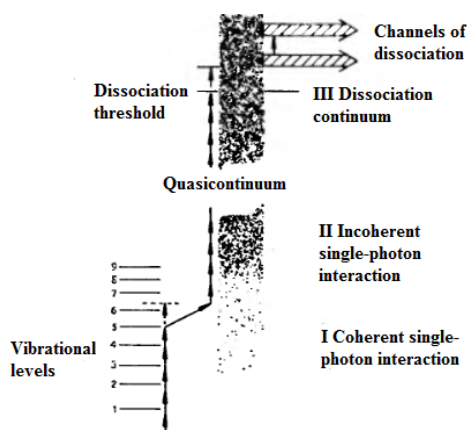


**Fig2.** Energy level diagram, which is corresponding the multiquantum infrared dissociation process. Coherent multiquantum interaction (Region I) is one of the methods of absorption in the zone of discrete vibrational levels. In the region of the quasicontinuum (CI), resonant absorptions are possible, and excitation is a stepwise process. The third region (III) lies above the dissociation region [2].

In this stage processes of absorption, which are resonanced to wavelength of laser radiation, are existed always, and therefore graduated transition is possible in region III, which are lying taller of dissociation threshold. After this the fast energy randomization with following monomolecule dissociation on fragments is realized [2].

Conditions of generation the multiharmonic in Nonlinear Optics are stronger as in the case of multiquantum dissociation. Main cause of this is crystal matrixes for centers of multiharmonic generation [4]. In firstly, concentration of centers the multiharmonic generation is  $\sim 10^{14} - 10^{16} \text{ cm}^{-3}$  [4] (impurity light absorption). Secondly, conditions of coherence (phase synchronism) leave the limitation on geometry of experiment: angles of phase synchronism are changed from  $\sim 10''$  to  $30'$  [4]. In this case (for initial radiation with wavelengths  $694.7 \text{ nm}$  and  $1024 \text{ nm}$ ) the vibrational part of spectrum gives negligible influence on these phenomena.

Conditions of phase synchronism are the conditions of spatial and temporal coherence in Nonlinear Optics. In this case, we must have generation of resonance homogeneous polarization. Differential photon efficiency may be changed from 0.1 percents to 50 percents [4].

The example of Nonlinear Optical phenomena with heterogeneous polarization is optical-induced Cherenkov radiation [7, 12]. Cherenkov radiation may be represented as radiating relaxation of optical-induced heterogeneous polarization of matter [7, 12]. Conditions of coherence for Cherenkov radiation have more complex nature as for classic Nonlinear Optics [7, 12].

The problem of laser radiation generation (saturation of the excitation of the corresponding radiative laser states) is related to the integral photon efficiency. The methods for achieving this state are different: from using resonators to increase feedback to explosions.

Let us illustrate the obtaining of positive feedback by the example of open cavities, which are used in pulsed solid-state lasers. The scheme of such a laser is shown in Fig. 3 [6].

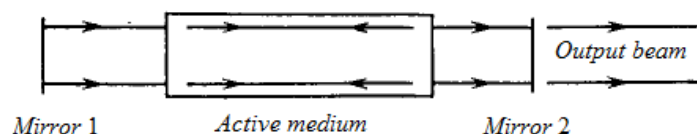


Fig3. Diagram of the laser device [6].

The resonator consists of two mirrors, one of which, in this case 2, is semitransparent. The resonator itself is tuned to the resonant frequency  $\nu$ , which is equal to the frequency of the laser radiation [6]. However, lasing is possible when threshold conditions are met. For a two-level system, the threshold condition for lasing is determined from the following relation

$$R_1 R_2 \exp[2\sigma(N_2 - N_1)l] = 1, \quad (2)$$

where  $R_1$  and  $R_2$  are light reflection coefficients of the first and second mirrors,  $\sigma$  is light absorption coefficient by the active medium,  $N_2 - N_1$  is the difference between the populations of the excited and ground states,  $l$  – the length of active medium.

Condition  $N_2 - N_1 > 0$  is called inversion condition, and the medium for which this condition is true is called active.

Condition (1) shows that the generation threshold is reached when the population inversion approaches a certain critical value  $(N_2 - N_1)_{cr}$  called the critical inversion and defined by the relation

$$(N_2 - N_1)_{cr} = -\ln(R_1 R_2) / 2\sigma l. \quad (3)$$

As soon as critical inversion is reached, generation will develop from spontaneous emission. Indeed, photons that are spontaneously emitted along the resonator axis will be amplified. This mechanism underlies the laser generator, usually called a laser [6].

This mechanism and implementation scheme is valid for a transparent medium with a concentration of laser radiation centers of  $10^{14} - 10^{17} \text{ cm}^{-3}$ . Therefore, these lasers have relatively low specific radiative photon efficiency per unit volume of the active medium. This characteristic is much greater for semiconductor injection lasers, since the emitter density there is practically equal to the semiconductor density  $\sim 10^{22} \text{ cm}^{-3}$  [21].

Now we must represent the holography as important chapter of modern optoelectronics [25-28]. Next chapters of of holography may be selected.

If Denisyuk hologram [27] is made three times using primary monochromatic radiation of three primary colors, then a color hologram will appear, and only a black-and-white result of interference will be recorded in the photographic emulsion. To record such holograms, special high-resolution (up to 5000 lines per millimeter) photographic emulsion has been developed. At the same time, it turned out that such emulsions have an extremely low photosensitivity (they can be irradiated with bright sunlight for a few seconds without fear of exposure), therefore, only recording can be carried out using an intense laser beam [25, 27].

D. Gabor created holography for the resolution problems of increasing resolving power of the electron microscopy [26]. He created classical scheme of two-beams holography. Further this method was developed for radiowaves by E. N. Leith and his colleagues and laser irradiation by E. N. Leith and J. Upatnieks [25]. These holograms were one and two-dimensional, Denisyuk ththree-dimensional [25, 27].

Differential efficiency of holograms is determined properties of the recording (recording) medium, and the integral one also by the conditions of irradiation both during their recording and during use [25-28].

#### 4. RELAXED OPTICS

Relaxed Optics [7-12] is a branch of modern physics that describes the processes of interaction between light and matter from the point of view of relaxation and evolution of the primary optical excitations of the medium. In a narrower sense, this section of physics describes the processes of irreversible interaction of light with a medium. The emergence of such a branch of physics is due to the development of laser technologies.

RO can be represented as the most complete formalization of I. Newton's phrase [29]: "The transitions of bodies into light and light into bodies obey the laws of nature, which seems to be amused by these transformations."

In general, RO is the synthesis of nonlinear optics, physical chemistry, radiation physics of a solid state, the physics of critical phenomena, etc., then, the natural problem of photon efficiency has a wider palette here than in sections 2 and 3 of this article, since here the phenomena are presented together, which are inherent in previously analyzed sciences. To confirm this, we present the relevant experimental data and models that were created to explain them in RO.

Firstly experimental data of irreversible interaction laser irradiation and InSb were received by V. Bogatyrev and G. Kachurin [30].

The profiles of a distribution of volume concentration of electrons in *InSb* after laser irradiation are represented in Fig. 4 [30]. These profiles were obtained by measuring the Hall effect using successive etching [30].

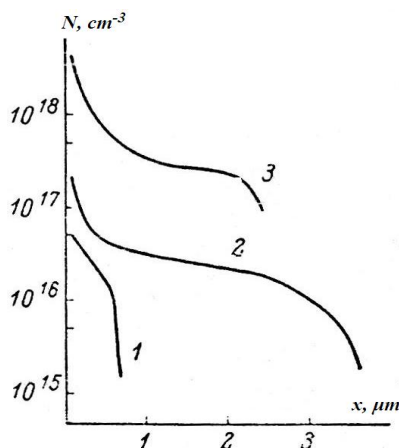


**Fig4.** Profiles of the volume distribution electrons after laser irradiation. 1, 2 – Ruby laser; 3 – YAG:Nd laser. Energy density in pulse,  $J/cm^2$ : 1 – 5; 2 – 40 [30].

An irradiation was created with help Ruby laser ( $\lambda = 0,69\mu\text{m}$ ,  $\tau_i = 5-6\text{ms}$ ) and series of impulses Nd:YAG laser ( $\lambda = 1,06\mu\text{m}$ ,  $\tau_i = 10\text{ns}$ , frequency of repetition of impulses was  $12,5\text{Hz}$ ). A value of threshold the energy of creation  $n$ -layers is equaled  $\sim 5\text{J}/\text{cm}^2$  for Ruby laser. A tendency of the saturation the layer concentration had place for the energy density  $\sim 30\text{J}/\text{cm}^2$  [30]. The melting of surface has place for this value of the irradiation.

The profiles of the distribution the photostimulated donor centers in subsurface layers *InSb* are represented in Fig. 5 [7, 8]. The samples of p-type conductivity are irradiated by pulses of Ruby laser (wavelength  $\lambda = 0,69\mu\text{m}$ , duration of pulse  $\tau_i = 20\text{ns}$ ). For intensity of irradiation  $I_0 > 0,001\text{J}/\text{cm}^2$  for *InSb* the  $n$ -layers on p-type materials are created. For intensity of irradiation  $I_0 < 0,1\text{J}/\text{cm}^2$  for *InSb* the profiles of the distribution of donor centers are represented the Buger-Lambert law (law of absorption the light in homogeneous media). For further increasing the irradiated intensity the profiles of the concentration donor centers have diffusion nature. The visible destruction of the irradiated semiconductor (melting, the change of the surface colour) had place for  $I_0 > 0,3\text{J}/\text{cm}^2$  for *InSb*.

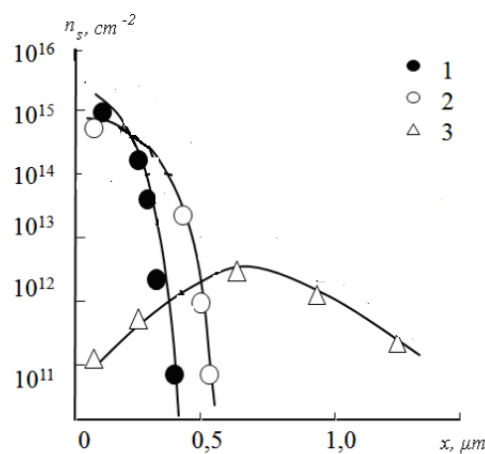


**Fig5.** The profiles of the distribution the layer concentration of the donor centers in inverse layers *InSb* after Ruby laser irradiation with various density of energy (monoimpulse regime): 0,07 (1); 0,1 (2); 0,16 (3)  $\text{J}/\text{cm}^2$  [7].

The created donor centers haven't temperature nature because thermodefacts in *InSb* has p-type conductivity [7-9]. The cause of the creations damages in our case is intensive explosion the pure covalent bonds in *InSb*. For these crystals the energy of these bond is equaled the energy of band gap  $E_g$  ( $0,18\text{eV}$  for *InSb* at room temperature). On Fig. 6 this bond is signed as 1. For one ions *In* and *Sb* is placed on minimal distance (the sum of corresponding covalent radiuses). Another chemical bonds in this crystal symmetry

Cross section of effective interaction the light quantum with bond 1 is more effective than for direction {110}. The angle among bond 1 and direction {110} is  $37,5^\circ$ . Quanta of ruby laser with another bonds are not interacted practically because it energy is less than energy of this bonds. The correlation effective squares of bond 1 for directions {110} and {111} are explained the corresponding experimental data [7-9].

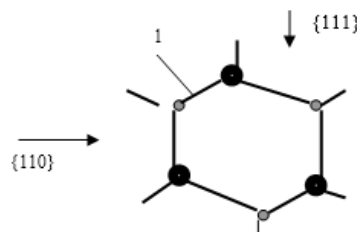


**Fig6.** Two-dimensional picture the crystal lattice  $A_3B_5$  (including *InSb*) of the cubic symmetry. Bond 1 is pure covalent [7-9].

The nature of the creation the damages may be next. For our correlation among quantum energy and  $E_g$  every quantum may break off 3-4 bonds of *InSb*. These results are corresponded the measurement

the temperature dependence of Hall's mobility in the temperature region 77-300<sup>0</sup>K [7-9]. The last allow associating donor centers and corresponding defects with vacancies or dislocations.

For the estimation the differential photochemical (photon) efficiency of using laser radiation for photochemical irreversible processes we can use next formula for the determination of number of broken chemical bonds per one photon  $n$  [7-9]

$$n = 2 \ln \frac{h\nu}{E_a}, \tag{4}$$

where  $h\nu$  – photon energy;  $E_a$  – energy of activation (broken) of corresponding bond.

So, for the case of the irradiation *InSb* by Ruby laser pulses (photon energy 1.78 eV) we have for the first bond of two-dimensional lattice of *InSb* ( $E_{1InSb} = 0.18$  eV) [3]. These crystals are direct-gap, so the band gap is equal to the energy of the minimum chemical bond [3]. Therefore,  $n_{InSb} \sim 4.6$  bonds/pulse. For case of irradiation *Si* ( $E_a \sim 1.6$  eV) by irradiation of eximer laser pulses (photon energy 5 eV) we have  $n_{Si} \sim 2.3$  bonds/pulse [31, 32]. These conditions allow increasing the lifetime of excited states and therefore the heating of irradiated matter may be negligible compared to direct photoionization, including phase transformations of the irradiated material.

Formula (1) has large value for the crystals. For the polymers, glasses and amorphous media this condition may be represented as [3]

$$h\nu > E_a. \tag{5}$$

These conditions may be supplemented by the multiphoton absorption conditions. But for the silicon we have more intensive generation of laser-induced surface structures for nanosecond irradiation by eximer *KrF*-laser [31, 32] as for femtosecond irradiation of laser with photon energy 1.55 eV [33].

For the determination the differential photochemical efficiency in addition to formulas (1) and (2), the excitation saturation procedure is of great importance.

In other words, for successive  $n$ -photon absorption for the next absorption event, the medium must be in the excited state that was obtained during previous absorptions.

In contrast to the formation of surface periodical structures three-dimensional periodic structures were obtained in this case. Focused laser irradiation with wavelength 800 nm and pulse duration 130 fs was used for the irradiation hexagonal silicon carbide 4H-SiC (Fig. 7). Sectional area of these structures was  $\sim 22 \mu\text{m}$ , the depth of  $\sim 50 \mu\text{m}$ . As seen from Fig. 7(c) we have five stages disordered regions, which are located at a distance from 2 to 4  $\mu\text{m}$  apart vertically [34, 35]. Branches themselves in this case have a thickness from 150 to 300 nm. In this case there are lines in the irradiated nanocavity spherical diameter of from 10 nm to 20 nm. In this case irradiated structures have crystallographic symmetry of the initial structure.

We see five groups of laser-induced damages (Fig. 7).

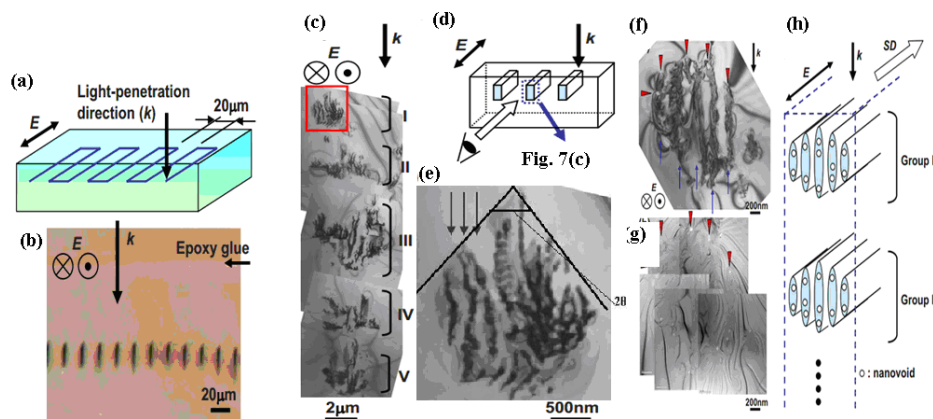


**Fig7.** (a) Schematic illustration of the laser irradiated pattern. The light propagation direction ( $k$ ) and electric field ( $E$ ) are shown. (b) Optical micrograph of the mechanically thinned sample to show cross sections of laser-

irradiated lines (200 nJ/pulse). (c) Bright-field TEM image of the cross section of a line written with pulse energy of 300 nJ/pulse. (d) Schematic illustration of a geometric relationship between the irradiated line and the cross-sectional micrograph. (e) Magnified image of a rectangular area in (c). Laser-modified layers with a spacing of 150 nm are indicated by arrows. (f) Bright-field TEM image of a portion of the cross section of a line written with pulse energy of 200 nJ/pulse. (g) Zero-loss image of a same area as in (f) with nanovoids appearing as bright areas. Correspondence with (f) is found by noting the arrowheads in both micrographs. (h) Schematic illustrations of the microstructure of a laser modified line. Light-propagation direction ( $k$ ), electric field ( $E$ ), and scan direction ( $SD$ ) are shown. Only two groups (groups I and II) of the laser-modified microstructure are drawn [34, 35].

In this case diffraction processes may be generated in two stages: 1 – formation of diffraction rings of focused beams [7] and second – formation of diffracting gratings in the time of redistribution of second-order Cherenkov radiation [7]. Second case is analogous to the creation of self-diffraction gratings in Nonlinear Optics, but for Fig. 7 (c) and Fig. 7 (g) our gratings are limited by Much cone of Cherenkov radiation.

For modeling of this experimental data next scenario was selected: focusing and equidistance diffraction stratification of initial laser beam; Cherenkov radiation in the cone of corresponding diffraction rings; interference of shortwave part of each Cherenkov cone. Microstructure of each groupe of laser-induced damages is result of optical breakdown in maximum of corresponding Cherenkov interferogramms [12]. Cherenkov angle was determined as additional to angle foci cone of initial radiation.

Volume density of energy of the creation focusing process may be determined with help next formula

$$W_{cvol} = E_a N_{nc}, \quad (6)$$

where  $E_a$  – energy of activation proper “nonlinear” centers;  $N_{nc}$  – their concentration.

Surface density for optical thin may be determined as

$$W_{csur} = W_{cvol} / \alpha, \quad (7)$$

where  $\alpha$  – absorbance index. Integral value of energy may be determined as

$$W_{crin} = W_{csur} \cdot S, \quad (8)$$

where  $S$  – the square of irradiation.

In this case

$$P_{cr} = W_{crin} / \tau_{ir}, \quad (9)$$

where  $\tau_{ir}$  is duration of laser irradiation.

The determination the concentration of scattering centers must be determined with conditions of proper experiment. It is determined by the conditions of observation the proper phenomena.

Next step of determination the density of energy in our cascade is condition of diffractive stratification. This condition may be determined with help of sizes the diffractive rings. We can estimate density of energy in plane of creation the diffractive stratification for  $n = 5$ .

The explanation of creation the laser-induced filaments have various interpretation. Firstly [7] is the creation wave-guide zones after point of collapse [7]. In this case filaments have little life-time.

Conic part of filament radiation has continuum spectrum: from ultraviolet to infrared. At first this effect was called superbroadening. Therefore it may be interpreted as laser-induced Cherenkov radiation [7]. The angle  $2\theta$  in the vertex of an angle of Fig. 7 (e) is double Cherenkov angle. In this case we have frozen picture of laser-induced destruction of 4H-SiC with help Cherenkov radiation.

The Cherenkov radiation is characterized by two peculiarities [7, 12]: 1) creation of heterogeneous shock polarization of matter and, 2) radiation of this polarization. The methods of receiving shock polarization may be various: irradiation by electrons,  $\gamma$ -radiation, ions and excitation with help pulse

fields. The stratification of this radiation on other type's radiation (volume, pseudo-Cherenkov a.o.) has relative character and may be represented as laser-induced Cherenkov radiation. Therefore in future we'll be represent conical part of filament radiation as Cherenkov [7, 12].

We can rough estimate basic peculiarities of energy distribution in Mach cone more precision formula as in [12]. This formula may be represented as

$$E_{lob} = \frac{\pi^2}{4} \left( \sum_{i=1}^5 n_{iav}^2 l_{iav} \right) r^2 N_{aSiC} E_{Zth}, \quad (10)$$

where  $n_{iav}$  – average visible number of filaments in proper group of cascade,  $l_{iav}=1000 \text{ nm}$  – average length of filaments in proper group of cascade,  $r = 10 \text{ nm}$  – average radius of filament,  $N_a$  – atom density of 4H-SiC,  $E_{Zth} \sim 25 \text{ eV}$  – Zeitz threshold energy for silicon carbide [12].

The atom density of 4H-SiC may be determined with help next formula

$$N_a = \frac{n\rho N_A}{A}, \quad (11)$$

where  $\rho$  – density of semiconductor,  $N_A$  – Avogadro number,  $A$  – a weight of one gram-molecule,  $n$  – number of atoms in molecule. For 4H-SiC  $N_{aSiC} = 9,4 \cdot 10^{21} \text{ cm}^{-3}$ .

For further estimation we use next approximation  $n_{1av} = n_{2av} = n_{3av} = n_{4av} = n_{5av} = 100$ , (see Fig. 7 (c)).

Energy, which is necessary for the optical breakdown our nanotubes may be determined in next way. Zeitz threshold energy for 4H-SiC is equaled  $E_{Zth} \sim 25 \text{ eV}$  [12]. Let this value is corresponded to energy of optical breakdown. Therefore summary energy  $E_{lob}$  is equaled

$$E_{lob} = N_{asnt} \cdot E_{Zth} = 23,2 \text{ nJ}. \quad (12)$$

This value is equaled of  $\sim 8\%$  from pulse energy or  $\sim 30\%$  from the effective absorbed energy of pulse. In this case we have differential photon efficiency, which show more high efficiency of transformation initial radiation to “irreversible” part of Cherenkov radiation. It is result of more intensive excitation comparatively with classical methods of receiving the Cherenkov radiation. In this case we have pure photochemical processes. The experimental data for intrinsic absorption (Fig. 7) show that for short pulse regime of irradiation (femtosecond regime) basic processes of destruction the fused silica and calcium fluoride are photochemical (multiphoton absorption in the regime of saturation the excitation). But basic peculiarity of experimental data Fig.7 is transformation the initial laser radiation (wavelength  $800 \text{ nm}$ ) to continuum Cherenkov radiation. From length of optical breakdown in 4H- SiC we can determine average absorption index of Cherenkov radiation. It is  $\sim 10^4 \text{ cm}^{-1}$ . This value is corresponded to violet-blue range of absorption spectrum of 4H-SiC. It is corresponded to ultraviolet and violet range of absorption spectrum of 4H- SiC [12].

We can estimate chain of critical value of energy for the 4H- SiC from physical-chemical point of view too.

Critical value of energy, which is necessary for the beginning of self-focusing, may be determined in next way. Volume density of energy of the creation self-focusing process may be determined with help formula (12). In further we made next approximation:  $E_a = h\nu = 1,5 \text{ eV}$ ;  $N_{nc} = (10^{14} - 10^{16}) \text{ cm}^{-3}$ .

Then we have for SiC  $W_{cvol} = 2,4 \cdot (10^{-5} - 10^{-3}) \text{ J/cm}^3$ . For SiC  $\alpha = 0,1 \text{ cm}^{-1}$ . And

$$W_{cstr} = 2,4 \cdot (10^{-4} - 10^{-2}) \text{ J/cm}^2.$$

Integral value of energy may be determined according by formula (6). For Fig. 7(c) for  $r = 2 \text{ }\mu\text{m}$ ,  $S = 1,256 \cdot 10^{-7} \text{ cm}^2$ . Therefore  $W_{crin} = 3(10^{-11} - 10^{-9}) \text{ J}$ . For  $r = 1 \text{ mm}$  we have  $W_{crin} = 1,9(10^{-6} - 10^{-4}) \text{ J}$ .

These estimations are corresponded to estimations, which are received with help formulas for Kerr media (electrodynamics formulas) [4]. For the gases this method allows to estimate the energy of its optical breakdown [12].

Next step of determination the density of energy in our cascade is condition of diffractive stratification. This condition may be determined with help of sizes the diffractive rings. We can estimate density of energy in plane of creation the diffractive stratification for  $n = 5$ .

Similar results were also obtained for the optical breakdown of potassium chloride upon irradiation with CO<sub>2</sub> laser pulses.

Two damages region in a crystal with moderately high density of inclusions were received in [36] for *KCl* after irradiation by CO<sub>2</sub>-lase pulses (wavelength 10,6 μm, duration of pulse 30 ns). The laser was known to be operating in the lowest-order transverse Gaussian mode. There were several longitudinal modes, however, which contributed a time structure to the pulse, periodic at the cavity round-trip time. The phase relationships between the longiotudional modes varied from shot to shot, changing the details of the time structure and causing the peak of the envelope to fluctuate by ±15% [36]. These results are presented in Fig. 8 [36].

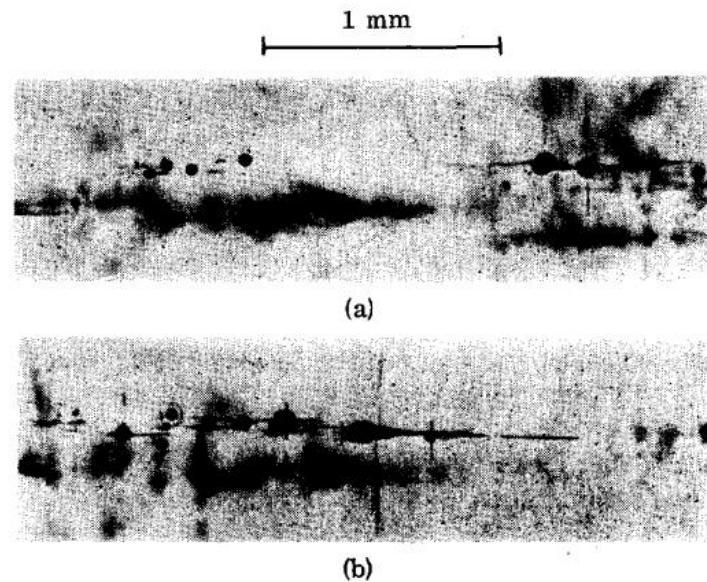


**Fig8.** Two damages region in a crystal *KCl* with moderately high density of inclusions. The round black objects are bubbles. The radiation, incident from left to right, was just at the intrinsic breakdown threshold. In one case (a) there was damage only at the inclusions. In (b), intrinsic breakdown occurred as evidenced by the pointed bubble. The straight lines represent cleavage [36].

The distance between diffraction spots and proper moving foci may be determined with help next formula

$$l_{nf} = \frac{d_{ndif}}{2 \tan \varphi/2} \tag{13}$$

where  $d_{ndif} = n\lambda$  is diameter of  $n$  diffractive ring,  $\lambda$  is wavelength of focusing light. The distances between bubbles of Fig. 7(b) are more as between regions of destruction of Fig. 7(c). But conditions of focusing the radiation in these both cases are equivalence. The distances between neighboring bubbles  $l_2$  of Fig. 8(b) and neighboring regions of destruction  $l_1$  of Fig. 7(c) are connected by next formula [12]

$$l_2 = \frac{d_{ndif2} \tan(\varphi_1/2)}{d_{ndif1} \tan(\varphi_2/2)} l_1 = \frac{\lambda_2 \tan(\varphi_1/2)}{\lambda_1 \tan(\varphi_2/2)} l_1 \tag{14}$$

In whole the correlation of this distasnces is depended from wavelength of irradiation and focusing angles, including intensity of irradiation? Which is determined the step o f homogeneity of irradiated matter. If we substitute in formula (14)  $\lambda_2 = 10,6 \mu m$  and  $\lambda_1 = 0,8 \mu m$  and  $\varphi_1 = \varphi_2$  then we'll receive

$$l_2 = 13,25 l_1 \tag{14a}$$

Energy characteristics of irradiation were represented in references on [36]. Therefore we select value 2 J/pulse from [12, 36]. In this case we have effective using energy. Methods of estimations of energy characteristics of *KCl* are rougher as for 4H-*SiC*. But we must suppose that focused laser irradiation has diffraction stratification, generation of Cherenkov radiation and interference of this Cherenkov

radiation. On Fig 8 (b) 5-7 steps of cascade optical breakdown we see. Sources of Cherenkov radiation and diffraction stratified cones.

The dependence of the distance between the groups of the cascade of laser-induced destruction on the wavelength of the incident radiation is confirmed experimentally:  $2 - 3 \mu\text{m}$  for silicon carbide and  $30 - 40 \mu\text{m}$  for potassium chloride.

The microstructure of destruction in the groups of the cascade for potassium chloride was not observed due to the low resolution of the photographic method ( $2 - 3 \mu\text{m}$ ), for electron microscopy –  $3 - 4 \text{ nm}$ .

If this scenario is true, we have as for 4H-SiC effective transformation the energy of laser radiation to cascade of laser-induced breakdown for KCl too. This value is 11,6 – 17,4 percents.

As we can see, the integral photon conversion efficiency of the initial radiation in this case is approximately the same as for silicon carbide.

Thus, in Relaxed Optics, the differential photon efficiency can be used to estimate the efficiency of using laser radiation at one of the stages of the cascade process of interaction of radiation with matter, and the integral efficiency can be used for part of proper cascade or the whole cascade, depending on the conditions of the problem being solved.

### 5. CONCLUSION

1. The short analysis the problem of photon efficiency in various forms in modern science is represented.
2. It was shown that photon efficiency may be having differential and integral nature.
3. The main concepts of photon efficiency are classified and a universal approach is developed on the basis of which this problem is analyzed in specific sciences.
4. Analysis of this problem in photochemistry was observed.
5. Generalized Stark-Einstein law was formulated.
6. Main peculiarities of photon efficiency Nonlinear Optics and Laser Physics are researched.
7. It was shown that in Relaxed Optics this problem has more complex nature as in other represented chapters of science.
8. Corresponding experimental data and models are represented and discussed.

### REFERENCES

- [1] Einstein A. (1913) Deduction thermodynamique de la loi de l'équivalence photochimique. J. Phys., ser. 5, vol. 111, 277-282 (in French)
- [2] Wayne R. P. (1988) Principles and Applications of Photochemistry. University Press, Oxford
- [3] Trokhimchuck P. P. (2022) Laser-induced sputtering (ablation) of matter: retrospective and perspective. IJARPS, vol. 9, is. 4, 10-33.
- [4] Shen Y. R. (2003) The principles of Nonlinear Optics. Wiley-Interscience, New York a. o.
- [5] Popescu I. M., Preda A. M., Cristescu C. P., Sterian P. E., Lupașcu A. I. (1975) Probleme rezolvate de fizica lazerilor. Editura tehnică, București (In Romanian)
- [6] Zvelto O. (2010) Principles of lasers. 5-th edition. Springer Verlag, Stuttgart
- [7] Trokhimchuck P. P. (2020) Relaxed Optics: Modeling and Discussions. Lambert Academic Publishing, Saarbrücken
- [8] Trokhimchuck P. P. (2012) Problem of saturation of excitation in relaxed optics. JOAM, vol. 7, is. 3-4, 363-370.
- [9] Trokhimchuck P. P. (2016) Relaxed Optics: Realities and Perspectives. Lambert Academic Publishing, Saarbrücken
- [10] Trokhimchuck P. P. (2021) Recent Research and Development Status of Relaxed Optics and Laser Technology: A Review. Optics and Photonics Journal, vol. 11, is. 7, 210-263.
- [11] Trokhimchuck P. P. (2020) Role Physical-Chemical Processes in the Generation of Laser-Induced Structures. In: Research Trends in Chemical Sciences, ed. Ashok Kumar Acharya, vol. 11, ch.6, AkiNik Publications, New Delhi, 109-140.
- [12] Trokhimchuck P. P. (2020) Laser-induced optical breakdown of matter: retrospective and perspective. Advances in Engineering Technology, Ed. Jaivir Singh, vol. 4, part 7. New Dehly, AkiNik Publications, 101-132

- [13] Zewail A. H. (1988) Laser Femtochemistry. *Science*, vol. 242, is. 4886, 1645-1653.
- [14] Semenov N. N. (1986) Chain reactions. Nauka, Moscow (In Russian)
- [15] Belousov B. P. (1959) Periodically acting reaction and its mechanism. Collection of abstracts on radiation medicine for 1958. Medgiz, Moscow, 145 (In Russian)
- [16] Zhabotinsky A. M. (1974) Concentration fluctuations. Nauka, Moscow (In Russian)
- [17] Murray J. (1977) Lectures on nonlinear-differential-equation models in biology. University Press, Oxford
- [18] Peter L. M. (2016) Chapter 1: Photoelectrochemistry: From Basic Principles to Photocatalysis, in *Photocatalysis: Fundamentals and Perspectives*, Royal Society of Chemistry, Cambridge, 1-28.
- [19] Calvert J. G., Pitts J. N. (1966) Photochemistry. John Wiley @ Sons, New York
- [20] Van 't Hoff Jacobus Henricus (Henry) (1884) *Etudes de dynamique chimique*. F. Muller und Co, Amsterdam (In French)
- [21] Gribkovskiy V. P. (1988) Semiconductor lasers. University Press, Minsk (In Russian)
- [22] Zhigarev A. A., Shamaeva G. T. (1982) Electron-beam and photoelectronic devices: Textbook for universities. Higher school, Moscow (In Russian)
- [23] Photochemistry and Reaction Kinetics. Eds. Ashmore P. G., Dainton F. S., Sugden T. M. (1967) Cambridge University Press, London
- [24] Zewail A. H. (1996) Femtochemistry: Recent progress in studies and control of reactions and their transitions states. *J. Phys. Chem.*, vol. 100, No.31, 12701 – 12724.
- [25] Caulfield H. J. (1979) Handbook of Optical Holography. Academic Press, New York
- [26] Gabor D. (1973) Holography (1948 – 1971). *Adv. Phys. Sc.*, vol. 109, is. 1, 1973, 5-30 (in Russian)
- [27] Denisjuk Yu. N. (1979) Principles of holography. Lectures. Sergey Vavilov optical institute, Leningrad (in Russian)
- [28] Baggioli M. (2019) Applied Holography. A Practical Mini-Course. SpringerBriefs in Physics. Springer Nature Switzerland AG, Cham
- [29] Newton I. (1730) *Opticks: or, A Treatise of the Reflexions, Refractions, Inflexions and Colours of Light*. Printer for William Innys at the Welt-End of St. Paul's, London
- [30] Bogatyryov V. A., Kachurin G. A. Physics and technical of semiconductors, v.11, No.1, 100-102. (In Russian).
- [31] Pedraza A. J., Fowlkes J. D. and Lowndes D. H. (1999) Silicon microcolumn arrays growth by nanosecond pulse laser irradiation. *Appl. Phys. Lett.*, vol. 74, is. 10, 2222-2224.
- [32] Pedraza A. J., Guan Y. F., Fowlkes J. D., Smith D. A. and Lowndes D. H. (2004) Nanostructures produced by ultraviolet laser irradiation of silicon. I. Rippled structures. *J. Vac. Sc. @ Techn. B.*, vol. 22, no.10, 2823-2835.
- [33] Shen M., Carey J. E., Crouch C. H., Kandyla M., Stone H. A., Mazur E. (2008) High-density regular arrays of nano-scale rods formed on silicon surfaces via femtosecond laser irradiation in water. *Nanoletters*, vol. 8, is. 7, 2087-2091.
- [34] Okada T., Tomita T., Matsuo S., Hashimoto S., Kashino R., Ito T. (2012) Formation of nanovoids in femtosecond laser irradiated single crystal silicon carbide. *Material Science Forum*, vol. 725, 19 – 22.
- [35] Okada T., Tomita T., Matsuo S., Hashimoto S., Ishida Y., Kiyama S., Takahashi T. (2009) Formation of periodic strain layers associated with nanovoids inside a silicon carbide single crystal induced by femtosecond laser irradiation. *J. Appl. Phys.*, v. 106, 054307, 5.
- [36] Yablonovich E. (1971) Optical Dielectric Strength of AlkaliHalide Crystals Obtained by Laserinduced Breakdown. *Appl. Phys. Lett.*, vol.19, is.11, 495-497.

**Citation:** Petro P. Trokhimchuck (2022) "Photon Efficiency: Retrospective and Perspective " *International Journal of Advanced Research in Physical Science (IJARPS)* 9(5), pp.1-14, 2022.

**Copyright:** © 2022 Authors, This is an open-access article distributed under the terms of the Creative Commons Attribution License, which permits unrestricted use, distribution, and reproduction in any medium, provided the original author and source are credited.